

\mathcal{PT} Metamaterials via Complex-Coordinate Transformation Optics

Giuseppe Castaldi,¹ Silvio Savoia,¹ Vincenzo Galdi,^{1,*} Andrea Alù,² and Nader Engheta³

¹*Waves Group, Department of Engineering, University of Sannio, I-82100 Benevento, Italy*

²*Department of Electrical and Computer Engineering,
The University of Texas at Austin, Austin, TX 78712, USA*

³*Department of Electrical and Systems Engineering,
University of Pennsylvania, Philadelphia, PA 19104, USA*

(Dated: October 30, 2012)

We extend the transformation-optics paradigm to a complex spatial coordinate domain, in order to deal with electromagnetic metamaterials characterized by balanced loss and gain, giving special emphasis to *parity-time* (\mathcal{PT}) symmetry metamaterials. We apply this general theory to complex-source-point radiation and unidirectional invisibility, illustrating the capability and potentials of our approach in terms of systematic design, analytical modeling and physical insights into complex-coordinate wave-objects and resonant states.

PACS numbers: 42.25.Bs, 42.70.-a, 11.30.Er

Balanced loss-gain artificial materials have elicited a growing attention in optics and photonics, mostly inspired by the emerging *parity-time* (\mathcal{PT}) symmetry concept, which was originally introduced in connection with quantum physics [1] (see [2] for a comprehensive review). Against the traditional axioms in quantum mechanics, Bender and co-workers [2] proved that even non-Hermitian Hamiltonians may exhibit *entirely real* energy eigenspectra, as long as they commute with the combined \mathcal{PT} -operator and share the same eigenstates. This implies, as a necessary condition on the quantum potential, $V(-\mathbf{r}) = V^*(\mathbf{r})$, with \mathbf{r} denoting a vector position and $*$ complex conjugation. The above condition is in general not sufficient, and it can be shown that there exists a critical non-Hermiticity threshold beyond which an abrupt phase transition occurs due to spontaneous \mathcal{PT} -symmetry breaking, and the eigenspectrum becomes (partially or entirely) *complex* [2]. This latter case is typically referred to as “broken” \mathcal{PT} symmetry, as opposed to the “full” \mathcal{PT} symmetry which is instead associated with real eigenspectra.

In view of the formal analogies between Schrödinger and paraxial Helmholtz equations, the above concepts and conditions may be straightforwardly translated to scalar optics and photonics scenarios, with complex-valued refractive-index profiles $n(-\mathbf{r}) = n^*(\mathbf{r})$ playing the role of the quantum potential. Such symmetry condition cannot be found in natural materials, but it may be engineered within current metamaterial technology, with a judicious spatial modulation of optical gain and losses (either along or across the propagation direction). Besides providing convenient experimental testbeds for \mathcal{PT} -symmetry-induced quantum-field effects that are still a subject of debate, \mathcal{PT} -symmetric metamaterials constitute *per se* a very intriguing paradigm, as the complex interplay between losses and gain may give rise to a wealth of anomalous, and otherwise unattainable, light-matter interaction effects that extend far beyond

the rather intuitive loss (over)compensation effects [3]. These include, for instance, double refraction [4], power oscillations [4, 5], spontaneous \mathcal{PT} -symmetry breaking [6, 7], beam switching [8], absorption-enhanced transmission [6], nonreciprocal propagation (e.g., “unidirectional invisibility”) [9–13], spectral singularities [14], and coherent perfect absorption [15, 16], with perspective applications to new-generation nonreciprocal optical components, switches, lasers, and absorbers.

In this Letter, we show that the *transformation optics* (TO) framework [17, 18] may be extended, via complex analytic continuation of the spatial coordinates, in order to deal with \mathcal{PT} -symmetric metamaterials. This extension brings along the powerful TO “bag of tools,” already applied successfully to a wide variety of field-manipulating metamaterials [19], in terms of systematic design, analytical modeling and valuable physical insights.

For simplicity, we start considering an auxiliary vacuum space with Cartesian coordinates $\mathbf{r}' \equiv (x', y', z')$, where time-harmonic $\exp(-i\omega t)$ electric (\mathbf{J}') and magnetic (\mathbf{M}') sources radiate an electromagnetic (EM) field (\mathbf{E}', \mathbf{H}'). We then consider a coordinate-transformation

$$\mathbf{r}' = \mathbf{F}(\mathbf{r}) \quad (1)$$

into a new *curved-coordinate* space. By relying on the covariance properties of Maxwell’s equations, the TO framework [18] allows for a “material” interpretation of the field-manipulation effects induced by the coordinate-transformation in (1), in terms of a new set of sources (\mathbf{J}, \mathbf{M}) and fields (\mathbf{E}, \mathbf{H}) residing in a *flat* physical space $\mathbf{r} \equiv (x, y, z)$ filled up by an inhomogeneous, anisotropic “transformation medium” (characterized by relative permittivity and permeability tensors $\underline{\underline{\epsilon}}$ and $\underline{\underline{\mu}}$, respectively)

that are related to the original quantities as follows

$$\{\mathbf{E}, \mathbf{H}\}(\mathbf{r}) = \underline{\underline{\Lambda}}^T(\mathbf{r}) \cdot \{\mathbf{E}', \mathbf{H}'\}[\mathbf{F}(\mathbf{r})], \quad (2a)$$

$$\{\mathbf{J}, \mathbf{M}\}(\mathbf{r}) = \det[\underline{\underline{\Lambda}}(\mathbf{r})] \underline{\underline{\Lambda}}^{-1}(\mathbf{r}) \cdot \{\mathbf{J}', \mathbf{M}'\}[\mathbf{F}(\mathbf{r})], \quad (2b)$$

$$\underline{\underline{\varepsilon}}(\mathbf{r}) = \underline{\underline{\mu}}(\mathbf{r}) = \det[\underline{\underline{\Lambda}}(\mathbf{r})] \underline{\underline{\Lambda}}^{-1}(\mathbf{r}) \cdot \underline{\underline{\Lambda}}^{-T}(\mathbf{r}). \quad (2c)$$

In (2), $\underline{\underline{\Lambda}} \equiv \partial(x', y', z')/\partial(x, y, z)$ indicates the Jacobian matrix of the transformation in (1), while the symbol $\det(\cdot)$ and the superscripts $^{-1}$ and $^{-T}$ denote the determinant, the inverse, and the inverse transpose, respectively. From (2c), it is evident that, in order for the resulting transformation medium to exhibit loss and/or gain, the coordinate transformation in (1) must be *complex-valued*. Complex-coordinate extensions of TO have already been explored in connection with single-negative transformation media [20] and field-amplitude control [21]. In the present investigation, although the framework can deal in principle with general (asymmetrical, unbalanced) loss-gain configurations, we focus on transformation media characterized by balanced loss and gain obeying the \mathcal{PT} -symmetry conditions.

First, it can be shown (see [22] for details) that the necessary condition $n(-\mathbf{r}) = n^*(\mathbf{r})$, usually considered in the scalar case to achieve \mathcal{PT} symmetry, can be generalized to our vector scenario as: $\underline{\underline{\varepsilon}}(-\mathbf{r}) = \underline{\underline{\varepsilon}}^*(\mathbf{r})$ [or, equivalently, $\underline{\underline{\mu}}(-\mathbf{r}) = \underline{\underline{\mu}}^*(\mathbf{r})$]. From (2c), we observe that such conditions are automatically fulfilled if the coordinate transformation in (1) is chosen so that

$$\underline{\underline{\Lambda}}(-\mathbf{r}) = \underline{\underline{\Lambda}}^*(\mathbf{r}). \quad (3)$$

Throughout, we use the general term “ \mathcal{PT} metamaterials” to indicate transformation media obtained using (2) that satisfy the condition in (3), i.e., that are characterized by either full or broken \mathcal{PT} -symmetry.

Our proposed TO framework allows the systematic synthesis [via (2c) and (3)] of \mathcal{PT} metamaterials, as well as the analytical modeling of their EM response [via (2a) and (2b)] and its physical interpretation in terms of analytically-continued complex-coordinate wave-objects residing in the auxiliary vacuum space. In what follows, for simplicity and without loss of generality, we focus on the two-dimensional (2-D) scenario illustrated in Fig. 1, featuring a slab-type configuration associated with the coordinate transformations

$$x' = xu(z), \quad y' = yv(z), \quad z' = w(z), \quad |z| \leq d. \quad (4)$$

As a first example of application, we illustrate a TO-based \mathcal{PT} -metamaterial realization of the *complex-source-point* (CSP) originally pioneered by Deschamps [23] and Felsen [24] during the 1970s, and widely utilized to construct new classes of *exact* field solutions which convert point/line-source-excited fields in a given environment into fields excited by Gaussian-beam-like wave objects in the same environment. In our example, we

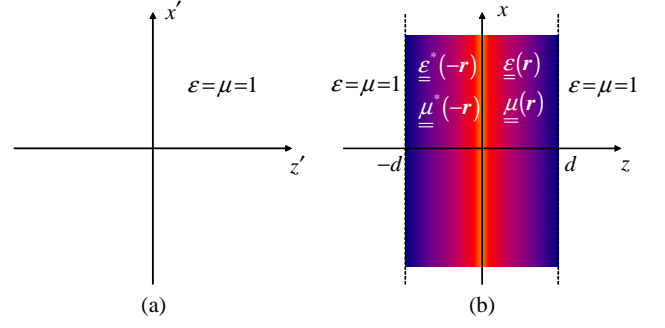


FIG. 1. (Color online) Problem schematic. (a) Auxiliary vacuum space. (b) Physical space with \mathcal{PT} -metamaterial slab, of thickness $2d$, associated with the coordinate transformations in (4).

consider a unit-amplitude (V/m), y -directed magnetic line-source centered at $x' = 0$ with a *purely imaginary* displacement along the z' axis,

$$M'_y(x', z') = \delta(x') \delta(z' - ib), \quad b > 0, \quad (5)$$

for which the y -directed radiated magnetic field can be obtained via analytic continuation of the well-known 2-D Green's function [25]

$$H'_y(x', z') = -\frac{\omega \varepsilon_0}{4} H_0^{(1)}(k_0 \tilde{s}'), \quad (6)$$

where $H_0^{(1)}$ denotes the zeroth-order Hankel function of first kind, $k_0 = \omega \sqrt{\varepsilon_0 \mu_0} = 2\pi/\lambda_0$ is the vacuum wavenumber (with λ_0 denoting the corresponding wavelength), and $\tilde{s}' = \sqrt{x'^2 + (z' - ib)^2}$, $\text{Re}(\tilde{s}') \geq 0$, represents a *complex distance*. This particular choice of branch-cut yields the so-called *source-type* solutions [24], associated with an equivalent source distribution occupying the region $|x'| < b$ in the real $z' = 0$ plane, and *discontinuous* across the same plane. This generates a wave-object that, within the paraxial regime (near the z' axis), is well-approximated by a Gaussian beam with diffraction length b propagating in the $z' > 0$ halfspace, with only weak radiation for $z' < 0$ (see [22] for details).

Here, we show that this radiation phenomenon may be envisioned and realized in a physically appealing TO-based \mathcal{PT} -metamaterial slab excited by a line-source placed in a real-coordinate point. This is based on a simple coordinate transformation (see [22] for details)

$$u(z) = v(z) = 1, \quad (7a)$$

$$w(z) = ib \left(1 \mp \frac{z}{d}\right), \quad \text{Re}(z) \geq 0, \quad |z| \leq d, \quad \text{Im}(z) = 0^+, \quad (7b)$$

which fulfills the conditions in (3) [22], and transforms [via (2b)] the original complex line-source (radiating in vacuum) into a conventional (real-coordinate) line-source embedded in a piecewise homogeneous \mathcal{PT} -metamaterial slab occupying the region $|z| \leq d$. For the

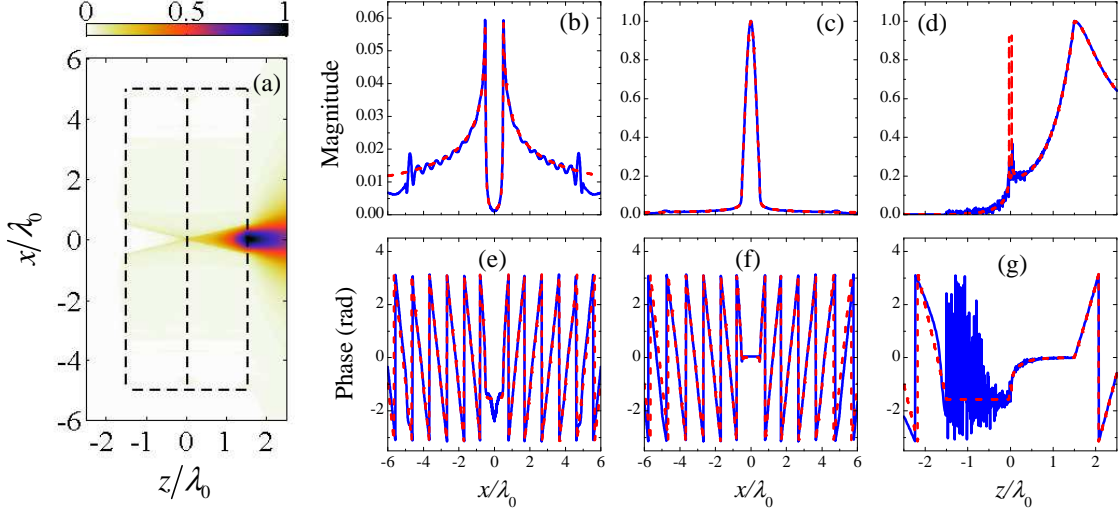


FIG. 2. (Color online) (a) Numerically-computed field magnitude ($|H_y|$) map pertaining to a \mathcal{PT} metamaterial slab of thickness $2d = 3\lambda_0$, transverse width $10\lambda_0$ (see dashed lines), and constitutive parameters as in (8) with $b = \lambda_0/2$ (i.e., $\varepsilon_{xx} = \mu_{yy} = \mp i/3$, $\varepsilon_{zz} = \pm 3i$, $z \geq 0$), excited by a magnetic line-source located at $x = z = 0$. (b), (c), (d) Transverse and longitudinal magnitude cuts (blue-solid curves) at $z = \mp(d + \Delta)$ and $x = \Delta$, respectively, with the small displacement $\Delta = \lambda_0/100$ added so as to avoid branch-point and source-related singularities. (e), (f), (g) Corresponding phase profiles. Also shown (red-dashed curves) are the TO-based theoretical predictions [infinite slab; cf. (2a) with (6)]. All field quantities are normalized with respect to $H_y(0, d)$.

assumed transverse-magnetic (TM) polarization, the relevant nonzero constitutive-tensor components are purely imaginary,

$$\varepsilon_{xx} = \mu_{yy} = \mp \frac{ib}{d}, \quad \varepsilon_{zz} = \pm \frac{id}{b}, \quad z \geq 0, |z| \leq d, \quad (8)$$

thereby representing a uniaxial zero-permittivity and zero-permeability metamaterial with balanced loss and gain. We stress that the chosen configuration serves only for illustrating, in the possibly simplest and more direct fashion, the general concept of metamaterial-induced wavefield “complexification,” which is a rather broad paradigm with a wealth of deep implications. Within this framework, no attempt was made to optimize the geometry and parameters so as to ensure the practical feasibility in a specific application scenario. In fact, from the application viewpoint, there are several alternative routes to converting an isotropic source to a collimated beam, with much simpler and application-ready implementations, without the need of resorting to \mathcal{PT} metamaterials. Nonetheless, in [22], we do address some implementation and practical feasibility issues in connection with the “exotic” media described in (8). The final result is a metamaterial that, when excited by a line source, produces the exact beam field distribution originally described by Deschamps [23] and Felsen [24] as a complex line source.

As an illustrative example, Fig. 2 shows the field map and representative cuts induced by a line source embedded in a \mathcal{PT} -metamaterial slab as in (8), with relevant

parameters given in the caption. For independent verification, we compare the theoretical TO-based predictions [cf. (2a) with (6)] with results from full-wave numerical simulations (see [22] for details) which also account for the finite extent (along x) of the slab. As can be observed, the agreement is very good, apart for some small numerical oscillations of the phase in a region where the field amplitude is negligibly small. From a physical viewpoint, these results nicely illustrate how the \mathcal{PT} -metamaterial slab can physically implement the complex-source displacement, reproducing at its interfaces $z = \pm d$ the two branches of a discontinuous equivalent source distribution in the real $z' = 0$ plane, continuously transitioning between them.

As a second illustrative example of the relevance of this complex-coordinate TO paradigm, we present a metamaterial slab supporting “unidirectional invisibility,” i.e., the existence of transmission resonances for which the reflectivity vanishes only for incidence from one side of the structure and not from the other. Though not necessarily restricted to \mathcal{PT} -symmetric scenarios, such nonreciprocal propagation phenomena [9–13] have recently elicited a significant attention and have been associated with the \mathcal{PT} -symmetry-breaking transition. In our example, we consider the coordinate transformation in (4) [subject to (3)] with

$$\begin{aligned} u(z) &= u_0^*, \quad v(z) = v_0^*, \quad w(z) = w_0^* z, \quad -d \leq z < 0, \\ u(z) &= u_0, \quad v(z) = v_0, \quad w(z) = w_0 z, \quad 0 < z \leq d, \end{aligned} \quad (9)$$

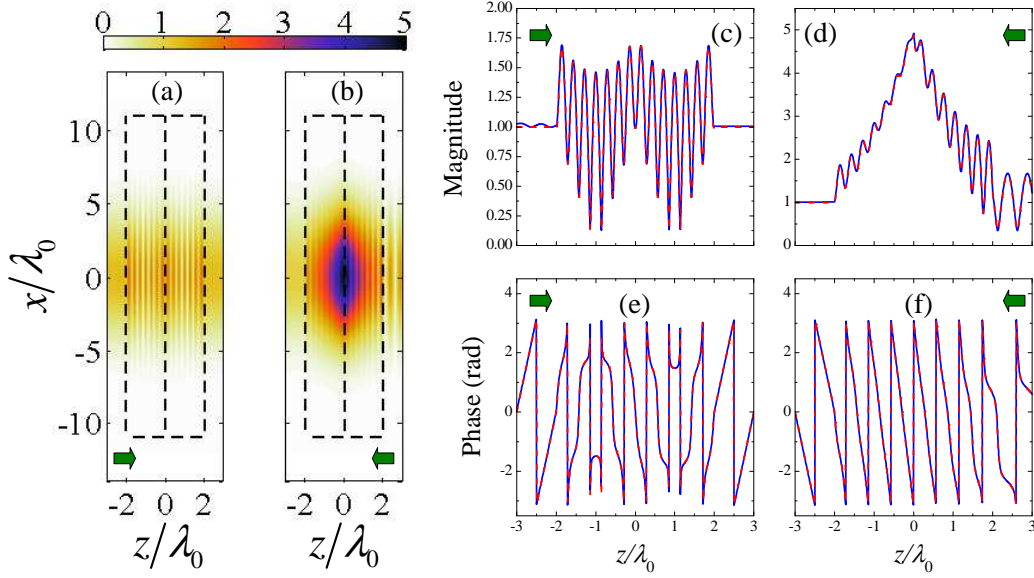


FIG. 3. (Color online) (a), (b) Numerically-computed field magnitude ($|H_y|$) maps pertaining to a \mathcal{PT} -metamaterial slab of thickness $2d = 4\lambda_0$, transverse width $22\lambda_0$ (see dashed lines), and constitutive parameters as in (8) with $u_0 = w_0 = 1.758 - 0.102i$ and $v_0 = 3.079 - 0.359i$ (i.e., $\varepsilon_{xx} = \varepsilon_{zz} = 3.079 \mp 0.359i$, $z \gtrless 0$, and $\mu_{yy} = 1$), excited by a unit-amplitude Gaussian beam with minimum waist of $4\lambda_0$ normally-incident from left and right, respectively (as schematically indicated by the thick arrows). (c), (d) Magnitude cuts (blue-solid curves) along the beam axis ($x = 0$), for incidence from left and right, respectively. (e), (f) Corresponding phase profiles. Also shown (red-dashed curves) are the TO-based theoretical predictions (infinite slab and plane-wave incidence) [22].

which yields a \mathcal{PT} -metamaterial slab as in Fig. 1. We consider a plane-wave illumination along the z -axis, with y -directed magnetic field

$$H_{iy}^{(l,r)}(z) = \exp(\pm ik_0 z), \quad (10)$$

with the l, r superscripts denoting incidence from left and right (i.e., $+$ and $-$ sign in the exponential), respectively. It is possible to analytically calculate the slab response by following the approach in [20] (see [22] for details). In particular, letting $H_{ry}^{(l,r)}$ and $H_{ty}^{(l,r)}$ the corresponding reflected and transmitted fields, respectively, we focus on the reflection ($R_{l,r}$) and transmission ($T_{l,r}$) coefficients for incidence from left and right,

$$R_l \equiv \frac{H_{ry}^{(l)}(-d)}{H_{iy}^{(l)}(-d)}, \quad R_r \equiv \frac{H_{ry}^{(r)}(d)}{H_{iy}^{(r)}(d)}, \quad (11a)$$

$$T_l \equiv \frac{H_{ty}^{(l)}(d)}{H_{iy}^{(l)}(-d)} = T_r \equiv \frac{H_{ty}^{(r)}(-d)}{H_{iy}^{(r)}(d)}. \quad (11b)$$

It can be shown (see [22] for details) that a sufficient condition for “invisibility from left” ($R_l = 0, T_l = 1$, i.e., zero reflection and no phase accumulation) is

$$v_0 = u_0 \left[i \tan \left(\frac{w_0 k_0 d}{2} \right) \right]^{\pm 1}, \quad (12)$$

where the ± 1 exponent identifies two distinct solutions. Under these conditions, we obtain for the reflection coefficient from right [22]

$$R_r = \pm 2 \text{Im} [\cos(w_0 k_0 d)]. \quad (13)$$

The relationships above depend in a remarkably simple fashion on the transformation parameters u_0 , v_0 and w_0 in (9) and the electrical thickness $k_0 d$, and provide useful insights into the effect of the complex-coordinate mapping. We note from (12) that solutions may exist only if $v_0 \neq \pm u_0$, which implies that the coordinate transformation in (9) needs to be *discontinuous*. As expected, for a *real* coordinate transformation, solutions may exist only for *complex* values of the electrical thickness $k_0 d$, which are *not physical*. Similar to the previous complex-source example, our complex-coordinate TO approach allows straightforward mapping of these physically-inaccessible solutions onto excitable resonant modes in a physical (real-coordinate) space. More specifically, for a given (real-valued) electrical thickness $k_0 d$ and a desired value of the reflection coefficient from right (R_r), we can obtain from (13) the required value of w_0 and subsequently, from (12), the ratio v_0/u_0 which identifies a *continuous infinity* of possible solutions. In particular, it is evident from (13) that, in order to attain *unidirectional* invisibility (i.e., $R_r \neq 0$) the transformation parameter w_0 needs simply to have nonzero real and imaginary parts.

Also in this case, the arising transformation medium is a piecewise homogeneous \mathcal{PT} -metamaterial slab,

$$\begin{aligned} \varepsilon_{xx} &= \frac{v_0^* w_0^*}{u_0^*}, \varepsilon_{zz} = \frac{v_0^* u_0^*}{w_0^*}, \mu_{yy} = \frac{u_0^* w_0^*}{v_0^*}, \quad -d \leq z < 0, \\ \varepsilon_{xx} &= \frac{v_0 w_0}{u_0}, \varepsilon_{zz} = \frac{v_0 u_0}{w_0}, \mu_{yy} = \frac{u_0 w_0}{v_0}, \quad 0 < z \leq d, \end{aligned} \quad (14)$$

which, for the assumed polarization, can be made effectively *nonmagnetic* (i.e., $\mu_{yy} = 1$) by enforcing $u_0 w_0 = v_0$, and *isotropic* ($\varepsilon_{xx} = \varepsilon_{zz}$) by enforcing $u_0 = \pm w_0$. This significantly simplifies the practical implementation, at the expense of reducing the degrees of freedom in the solutions, which are now related to the (countably infinite) roots of the transcendental equations

$$w_0 = \left[i \tan \left(\frac{w_0 k_0 d}{2} \right) \right]^{\pm 1}, \quad (15)$$

without direct control of R_r in (13).

Figure 3 shows the numerically-computed [22] field maps and relevant field cuts (blue-solid curves) for a Gaussian-beam exciting a nonmagnetic, isotropic, truncated \mathcal{PT} -metamaterial slab with moderate thickness ($2d = 4\lambda_0$) and $\varepsilon_{xx} = \varepsilon_{zz} = 3.079 \mp 0.359i$, $z \geq 0$. It is fairly evident the strong difference between the responses pertaining to incidence from left [nearly-zero reflection with no phase accumulation; cf. Figs. 3(a), 3(c) and 3(e)] and right [sensible reflection ($|R_r| \approx 0.33$); cf. Figs. 3(b), 3(d) and 3(f)]. Once again, these results are in very good agreement with the TO-based theoretical predictions (red-dashed curves) for infinite slab and plane-wave excitation. Also in this case, the parameters were mainly chosen for the sake of simplicity of illustration and visualization, and the resulting gain levels required are probably unrealistic within current technology. However, we did verify that lower levels of loss/gain may be traded-off for larger electrical-thickness values. For instance, loss/gain-tangent values of $\sim 10^{-2}$ and $\sim 10^{-3}$ may be attained for thickness values $d \sim 200\lambda_0$ and $\sim 2000\lambda_0$, respectively, which may be of practical interest for optical wavelengths.

In conclusion, we have shown that complex-coordinate TO may be exploited for systematic generation, design and modeling of \mathcal{PT} metamaterials for a variety of applications. As illustrated in our examples, the most attractive and interesting aspect of the proposed approach is the metamaterial-based transposition to an actual physical space of wave-objects and resonant states residing in complex-coordinate spaces. Given the power and pervasiveness of analytic-continuation approaches in wave-physics, this is expected to open up a plethora of new

intriguing venues for \mathcal{PT} metamaterials. Accordingly, current and future studies are aimed at exploring more general transformation classes, as well as different geometries (e.g., cylindrical and spherical) and applications.

A.A. acknowledges the support of Dr. Arje Nachman under the AFOSR YIP Grant No. FA9550-11-1-0009.

* vgaldi@unisannio.it

- [1] C. M. Bender and S. Boettcher, Phys. Rev. Lett. **80**, 5243 (1998).
- [2] C. M. Bender, Rep. Prog. Phys. **70**, 947 (2007).
- [3] S. Xiao, V. P. Drachev, A. V. Kildishev, X. Ni, U. K. Chettiar, H.-K. Yuan, and V. M. Shalae, Nature (London) **466**, 735 (2010).
- [4] K. G. Makris, R. El-Ganainy, D. N. Christodoulides, and Z. H. Musslimani, Phys. Rev. Lett. **100**, 103904 (2008).
- [5] M. C. Zheng, D. N. Christodoulides, R. Fleischmann, and T. Kottos, Phys. Rev. A **82**, 010103(R) (2010).
- [6] A. Guo, G. J. Salamo, D. Duchesne, R. Morandotti, M. Volatier-Ravat, V. Aimez, G. A. Siviloglou, and D. N. Christodoulides, Phys. Rev. Lett. **103**, 093902 (2009).
- [7] C. E. Rüter, K. G. Makris, R. El-Ganainy, D. N. Christodoulides, M. Segev, and D. Kip, Nature Phys. **6**, 192 (2010).
- [8] A. A. Sukhorukov, Z. Y. Xu, and Y. S. Kivshar, Phys. Rev. A **82**, 043818 (2010).
- [9] H. Ramezani, T. Kottos, R. El-Ganainy, and D. N. Christodoulides, Phys. Rev. A **82**, 043803 (2010).
- [10] Z. Lin, H. Ramezani, T. Eichelkraut, T. Kottos, H. Cao, and D. N. Christodoulides, Phys. Rev. Lett. **106**, 213901 (2011).
- [11] Li Ge, Y. D. Chong and A. D. Stone, Phys. Rev. A **85**, 023802 (2012).
- [12] A. Regensburger, C. Bersch, M.-A. Miri, G. Onishchukov, D. N. Christodoulides, and U. Peschel, Nature (London) **488**, 167 (2012).
- [13] A. Mostafazadeh, arXiv:1206.0116v1 [math-ph] (2012).
- [14] A. Mostafazadeh, Phys. Rev. Lett. **102**, 220402 (2009).
- [15] S. Longhi, Phys. Rev. A **82**, 031801(R) (2010).
- [16] Y. D. Chong, Li Ge, and A. D. Stone, Phys. Rev. Lett. **106**, 093902 (2011).
- [17] U. Leonhardt, Science **312**, 1777 (2006).
- [18] J. B. Pendry, D. Schurig, and D. R. Smith, Science **312**, 1780 (2006).
- [19] H. Chen, C. T. Chan, and P. Sheng, Nature Materials **9**, 387 (2010).
- [20] G. Castaldi, I. Gallina, V. Galdi, A. Alù, and N. Engheta, J. Opt. **13**, 024011 (2011).
- [21] B.-I. Popa and S. A. Cummer, Phys. Rev. A **84**, 063837 (2011).
- [22] Supplementary material, available online at <http://tinyurl.com/8kzzph3>.
- [23] G. A. Deschamps, Electron. Lett. **7**, 684 (1971).
- [24] L. B. Felsen, Symp. Math. **18**, 39 (1976).
- [25] L. B. Felsen and N. Marcuvitz, *Radiation and Scattering of Waves* (IEEE-Wiley, Piscataway, NJ, 1994).